NUMERICAL SIMULATION OF CHEMOTAXIS MODELS ON STATIONARY SURFACES

ANDRIY SOKOLOV*, ROBERT STREHL*, AND STEFAN TUREK*

Abstract. In this paper we present an implicit finite element method for a class of chemotaxis models, where a new linearized flux-corrected transport (FCT) algorithm is modified in such a way as to keep the density of on-surface living cells nonnegative. Level set techniques are adopted for an implicit description of the surface and for the numerical treatment of the corresponding system of partial differential equations. The presented scheme is able to deliver a robust and accurate solution for a large class of chemotaxis-driven models. The numerical behavior of the proposed scheme is tested on the blow-up model on a sphere and an ellipsoid and on the pattern-forming dynamics model of *Escherichia coli* on a sphere.

Key words chemotaxis model, pattern formation, FEM, FCT, level set

1. Introduction. After first being introduced in the beginning of the seventies by E. Keller and L. Segel [24, 25] for modeling the behavior of the slime mold amoeba *Dictyostelium discoideum*, chemotaxis models became widely used in many medical and biological applications. Among them are bacteria/cells aggregation and pattern formation processes [1, 32, 42, 43, 44] and modeling of tumor invasion and metastasis processes before a proliferation dominated stage [4, 6, 7, 8, 9], modeling of vasculogenesis [3, 19, 37], which is very important for understanding tissue engineering and regeneration, etc.
Many interesting mathematical questions arise also in the context of the chemotaxis-driven systems. The main point is the existence and uniqueness of the solution. In particular, unbounded aggregation of cells may give rise to singularities at accumulation points. This phenomenon is known as the *blow-up* effect [34, 21, 33, 36, 22, 11, 12, 23]. Another interesting phenomenon is the fact that a homogeneous stationary solution may become unstable for large values of the chemotactic sensitivity function $\chi(\cdot)$ under some conditions on the reactive source term in the chemotactic growth system. Such instabilities may give rise to rapidly evolving transient solutions and/or special patterns which are observed in biological experiments (see, e.g. [1, 2]) and were already mentioned above.
From the numerical point of view, one of the main problems to be dealt with is due to the rapid growth of solutions in a small neighborhood of certain points or curves. In particular, the blow-up phenomenon or a singular spiky behavior of exact solutions may give rise to nonphysical oscillations if the employed numerical scheme is not guaranteed to satisfy the discrete maximum principle (DMP). The construction process of a nonoscillatory, positivity-preserving, accurate numerical scheme for chemotaxis-like problems can be compared with the numerical stabilization of advection dominated problems in Computational Fluid Dynamics (CFD). It is known that an adequate treatment of unstable advective terms is a matter of utmost importance for the majority of CFD applications.

In the last decade several methods for the numerical treatment of the chemotactic term $\nabla\cdot(A(u)\,B(c)\,C(\nabla c))$ (mostly applicable to its simplified form $\nabla\cdot(\chi\,u\nabla c)$), where u is the cell density and c is the chemoattractant, have been proposed. Chertock and Kurganov [10] proposed a second-order Godunov-type central-upwind scheme for chemotaxis and haptotaxis systems and related models. The constructed scheme belongs to the class of finite-volume methods and was proven to preserve the positivity of the cell density. Numerical

*Institut für Angewandte Mathematik, TU Dortmund, 44227 Dortmund, Germany
(asokolow@math.tu-dortmund.de, robert.strehl@tu-dortmund.de, ture@featflow.de).

results were obtained for the 2D case on unit square geometries. Another finite-volume approach for the Keller-Segel chemotaxis model is due to Filbet [16]. He also studied an implicit upwind-like numerical scheme and carefully analyzed it to understand if it gives the correct behavior of the solution when it is effectively smooth and when it blows up. Tyson *et al.* proposed a fractional step method for the partial differential equations arising in the chemotaxis models [44]. In every time step the solution procedure was split up into three independent steps corresponding to the advection, diffusion and reaction processes. Each step was handled independently using the finite-volume discretization in space. The advection step was solved with the help of the CLAWPACK simulation tool [31], which incorporates the 'flux-limiting' stabilization strategy. For the diffusion step the A-stable and L-stable TR-BDF2 method was used. There are also attempts by H. Gajewski *et al.* to develop numerical software for chemotaxis problems [17, 18].

Among finite element approximations for the nonlinear chemotaxis system one can find a method proposed by Saito in [35]. Herein he utilizes an upwind technique to construct a numerical scheme that satisfies both positivity and mass conservation properties. The discontinuous Galerkin methods, so popular in the numerical community since the late nineties, were accommodated for the Keller-Segel chemotaxis system by Epshteyn and Kurganov, see [14, 15]. Their methods are based on three primal discontinuous Galerkin methods: Nonsymmetric Interior Penalty Galerkin, Symmetric Interior Penalty Galerkin and Incomplete Interior Penalty Galerkin. The numerical fluxes for the approximation of the advective term employ a central-upwind scheme, which belongs to *the family of nonoscillatory central schemes, applicable to general multidimensional systems of conservation laws and related problems*. Developed by Kuzmin, Turek *et al.*, the Flux-Corrected Transport (FCT) and FEM-TVD algorithms for unstructured meshes were explored for the chemotaxis models in two- and three space dimensions, see [38, 39]. They were shown to be accurate and positivity-preserving, even in the case of solutions with sharp peaks that blow-up in the center or at the boundary of the domain.

Though mathematical analysis of chemotaxis models and analysis of evolving in time manifolds started already several decades before, their integration occurred just recently due to the necessity of constructing complex models for biological and medical applications. Very often one has to couple PDEs defined in a domain with PDEs defined only on some manifold (one can think, e. g., of a cell membrane). At the same time the modeled processes might lead to the shape deformation of the manifold. As one of the first works for chemotaxis-driven processes on surfaces we would like to mention the paper by Voigt *et. al.* [46], where the chemotaxis of bone marrow-derived mesenchymal stem cells is simulated, and by Elliott *et. al.* [45], where the shape of a single cell evolves due to its chemotaxis response.

In this article we describe a special numerical scheme for chemotaxis-like models, which makes it possible to couple partial differential equations on a surface with those, which are defined on some embedded into this domain manifold. The article is organized as follows: in section 2 we define the problem. Then, in section 3, subsection 3.1, we describe the level set methodology: numerical treatment of the Laplace-Beltrami term and of the on-surface defined advective term. After that in subsection 3.2 we present the modified FCT-stabilization technique for on-surface defined advection-dominated equations. In section 4 we demonstrate numerical results for blow-up problems on a sphere and on an ellipsoid. Then, we consider a more realistic chemotaxis model, where a pattern forming behavior of bacteria along a sphere occurs due their response to the chemoattractant, which is distributed in the surrounding domain. Section 5 summarizes the characteristics of the proposed approach.

2. Problem formulation. Almost all chemotaxis models, which were mentioned in the previous section can be mathematically described by the following system of reaction-advection-diffusion equations:

$$\frac{\partial u_i}{\partial t} = D_i^u \Delta u_i + \nabla \cdot [\boldsymbol{\chi}_i^u \cdot \boldsymbol{v}_i^u(\boldsymbol{u}, \boldsymbol{c}, \boldsymbol{\rho}) u_i] + f_i(\boldsymbol{u}, \boldsymbol{c}, \boldsymbol{\rho}), \quad \text{in } \Omega \times T, \tag{2.1}$$

$$\frac{\partial c_j}{\partial t} = D_j^c \Delta c_j - \sum_{k=1}^{m} \alpha_{k,j} c_k + \sum_{k=1}^{n} \beta_{k,j} u_k + g_j(\boldsymbol{u}, \boldsymbol{c}, \boldsymbol{\rho}), \quad \text{in } \Omega \times T \tag{2.2}$$

$$\frac{\partial \rho_l}{\partial t} = D_l^\rho \Delta_\Gamma \rho_l + \nabla_\Gamma \cdot (\boldsymbol{\chi}_l^\rho \cdot \boldsymbol{v}_l^\rho(\boldsymbol{u}, \boldsymbol{c}, \boldsymbol{\rho}) \rho_l) + s_l(\boldsymbol{u}, \boldsymbol{c}, \boldsymbol{\rho}), \quad \text{on } \Gamma \times T \tag{2.3}$$

with corresponding boundary and initial conditions. Here, $u_i(t, \boldsymbol{x})$, $i = 1 \dots n$, denotes densities of species, which live in a bounded domain $\Omega \subset \mathbb{R}^d$, $d = 2, 3$, $c_j(t, \boldsymbol{x})$, $j = 1 \dots m$, stands for concentration of chemoattractants and $\rho_l(t, \boldsymbol{x})$, $l = 1 \dots p$, are densities of species, which live on a closed smooth surface Γ. Velocities $\boldsymbol{v}$ in equations (2.1) and (2.3) can describe the species-chemoattractant interaction ($\boldsymbol{v} = \nabla c$), species-species interaction $\boldsymbol{v} = \nabla u$ or some external velocity (e.g., due to fluid flow, evolution of a surface, etc.). $\boldsymbol{\chi}^u$ and $\boldsymbol{\chi}^\rho$ are vectors of chemo-, resp. chemosensitivity entries, which can be nonlinear. We distinguish two cases. In the first case, see Figure 2.1 (a), $\Gamma \subset \Omega$. Here, we introduce a narrow band $\Omega_\Gamma \subset \Omega$ around Γ, where the equation (2.3) is treated by the level set method. In the second case, see Figure 2.1 (b), $\Gamma = \partial\Omega$ and we take Ω_Γ to be a narrow band in a direction, which is opposite to outer-normal of $\partial\Omega$. In both cases the computational domain is Ω. This procedure allows us to perform the direct coupling of domain-defined equations (2.1)–(2.2) with a surface-defined equation (2.3).

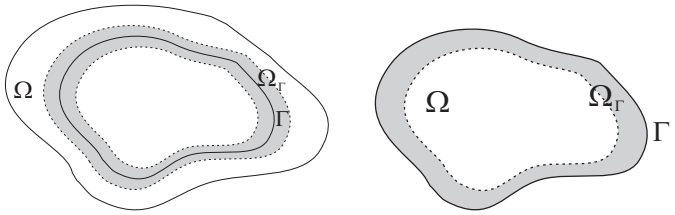

FIG. 2.1. *(left)* $\Gamma \subset \Omega$, *(right)* $\Gamma = \partial\Omega$.

In a series of papers [38, 39, 40] the authors constructed a robust and efficient numerical scheme for chemotaxis problems in 2 and 3 spatial dimensions, in the case when $n = 1$, $m = 1$ and $p = 0$. There, the FCT-TVD stabilization techniques, Newton-like solvers and coupled, resp., decoupled approaches were analyzed. It was shown that the solver was able to deliver physically appropriate and accurate numerical solutions. Using the FCT method and the operator splitting technique one can extend the proposed framework to the case of multi-species and multi-chemos. In this paper we construct a numerical scheme for the equation (2.3) and couple this equation with the chemotaxis system (2.1)–(2.2). The surface Γ is considered to be stationary. From the analytical point of view one does not know, how curvature of a manifold influences blow-up: are blow-up points at points of largest curvature, is blow-up quicker if curvature is larger, etc? For this reason, we consider some numerical experiments for chemotaxis problems on surfaces of constant and varying curvature. The developed scheme and numerical results provide a promising basis for further studies in this context.

3. Numerical scheme. The construction of positivity preserving, robust numerical schemes for the system (2.1)–(2.2) was thouroughly analyzed in [38, 39]. Therefore, here

we focus on the equation (2.3). Let us rewrite it in the following form

$$\frac{\partial \rho}{\partial t} = D\Delta_\Gamma \rho + \nabla_\Gamma \cdot (\boldsymbol{v}\rho) + s, \tag{3.1}$$

where $\Delta_\Gamma \rho$ is the Laplace-Beltrami term and $\nabla_\Gamma \cdot (\boldsymbol{v}\rho)$ is the on-surface defined advective term. For the simplicity of notation we set $\Omega_\Gamma = \Omega$ and use the symbol Ω to denote both domains. We also assume that ρ^* is a natural extension of ρ from Γ to the whole domain Ω. In the following we will omit $*$ and will write simply ρ. The two main points, which we consider in details are the treatment of the surface-defined terms and the corresponding application of the FCT stabilization technique to the discretized $\nabla_\Gamma \cdot (\boldsymbol{v}\rho)$ term.

3.1. Level set: diffusion and advection on a surface. To obtain the semi-discrete form for equation (3.1) we adopt the level set method. We assume that Γ is a compact smooth connected and oriented hypersurface in $\mathbb{R}^d$ and that there exists a smooth level set function

$$\phi(\boldsymbol{x}) = \begin{cases} < 0 & \text{if } \boldsymbol{x} \text{ is inside } \Gamma \\ 0 & \text{if } \boldsymbol{x} \in \Gamma \\ > 0 & \text{if } \boldsymbol{x} \text{ is outside } \Gamma \end{cases} \tag{3.2}$$

such that $|\nabla\phi| \neq 0$. Then, an outward normal to Γ is

$$\boldsymbol{n} = (n_i)_i = \nabla\phi/|\nabla\phi| \tag{3.3}$$

and

$$\mathcal{P}_\Gamma = (\delta_{ij} - n_i n_j)_{ij} = I - \frac{\nabla\phi}{|\nabla\phi|} \otimes \frac{\nabla\phi}{|\nabla\phi|} \tag{3.4}$$

is the projection onto the tangent space $\mathcal{T}_{\boldsymbol{x}}\Gamma$. Observe that if $\phi(\cdot)$ is chosen as a signed distance function then $|\nabla\phi| = 1$. For a scalar function ξ on Ω and a tangential vector field $\boldsymbol{\xi}$ on Γ one obtains

$$\nabla_\Gamma \xi = \left(\frac{\partial \xi}{\partial x_i} - n_i n_j \frac{\partial \xi}{\partial x_j} \right)_i, \tag{3.5}$$

$$\nabla_\Gamma \cdot \boldsymbol{\xi} = \frac{\partial \xi_i}{\partial x_i} - n_i n_j \frac{\partial \xi_i}{\partial x_j}. \tag{3.6}$$

Therefore the Laplace-Beltrami operator on Γ with respect to the level set function ϕ can be written as

$$\Delta_\Gamma \xi = \nabla_\Gamma \cdot \nabla_\Gamma \xi = \nabla \cdot \mathcal{P}_\Gamma \nabla \xi. \tag{3.7}$$

From the Coarea's formula [13] it is known that

$$\int_{\inf_\Omega \phi}^{\sup_\Omega \phi} \left(\int_{\Gamma_r} \xi \right) d\, r = \int_\Omega \xi |\nabla\phi|, \tag{3.8}$$

where $\Gamma_r = \{\boldsymbol{x} | \phi(\boldsymbol{x}) = r\}$. After multiplying the equation (3.1) by finite element test functions $\{\varphi\}$ and integrating over Ω, we obtain a weak formulation for (3.1):

$$\frac{\partial}{\partial t} \int_\Omega \rho\varphi|\nabla\phi| = \int_\Omega D\Delta_\Gamma \rho\varphi|\nabla\phi| + \int_\Omega \nabla_\Gamma \cdot (\boldsymbol{v}\rho)\varphi|\nabla\phi| + \int_\Omega s\varphi|\nabla\phi| \tag{3.9}$$

The Eulerian integration by parts (see, e.g., [13]) applied to the Laplace-Beltrami term on the right hand side of (3.9) together with the assumption

$$\int_\Omega \nabla_\Gamma \cdot (D\nabla_\Gamma \rho\varphi)|\nabla\phi| = \int_{\partial\Omega} D\nabla_\Gamma \rho \cdot \boldsymbol{n}_\Omega \varphi|\nabla\phi| = 0,$$

where $\boldsymbol{n}_\Omega$ is a normal to $\partial\Omega$, give us

$$\begin{aligned}\int_\Omega D\nabla_\Gamma \rho \cdot \nabla_\Gamma \varphi|\nabla\phi| &= -\int_\Omega \nabla_\Gamma \cdot D\nabla_\Gamma \rho\varphi|\nabla\phi| + \int_\Omega \nabla_\Gamma \cdot (D\nabla_\Gamma \rho\varphi)|\nabla\phi| \\ &= -\int_\Omega \nabla_\Gamma \cdot D\nabla_\Gamma \rho\varphi|\nabla\phi| \end{aligned} \tag{3.10}$$

or, due to (3.4),

$$\int_\Omega \nabla_\Gamma \cdot D\nabla_\Gamma \rho\varphi|\nabla\phi| = -\int_\Omega D\mathcal{P}_\Gamma \nabla\rho \cdot \nabla\varphi|\nabla\phi|. \tag{3.11}$$

The advective term $\nabla_\Gamma \cdot (\boldsymbol{v}\rho)$ is treated in a similar way. Namely, applying the Eulerian integration by parts to the corresponding weak formulation of $\nabla_\Gamma \cdot (\boldsymbol{v}\rho)$, one obtains:

$$\int_\Omega \nabla_\Gamma \cdot (\boldsymbol{v}\,\rho)\varphi|\nabla\phi| = -\int_\Omega \rho\,\boldsymbol{v} \cdot \nabla_\Gamma \varphi|\nabla\phi| + \int_{\partial\Omega} \boldsymbol{v} \cdot \boldsymbol{n}_{\partial\Omega} \rho\varphi|\nabla\phi|. \tag{3.12}$$

In general, the integral along the boundary on the right hand side of (3.12) can bring sufficient changes into the solution dynamics and therefore cannot be neglected, see, e.g., [26]. Assuming that $\partial\Omega$ is aligned along Γ_c, for some c, and setting some restrictions on $\boldsymbol{v}$, we can write

$$\int_{\partial\Omega} \rho\,\boldsymbol{v} \cdot \boldsymbol{n}_{\partial\Omega} \varphi|\nabla\phi| = 0. \tag{3.13}$$

Therefore

$$\int_\Omega \nabla \cdot (\rho\,\boldsymbol{v})\varphi|\nabla\phi| = -\int_\Omega \rho\,\boldsymbol{v} \cdot \nabla_\Gamma \varphi|\nabla\phi|, \tag{3.14}$$

and the resulting semi-discrete scheme looks as follows:

$$\frac{\partial}{\partial t}\int_\Omega \rho|\nabla\phi| + \int_\Omega D\mathcal{P}_\Gamma \nabla\rho \cdot \nabla\varphi|\nabla\phi| - \int_\Omega \rho\,\boldsymbol{v} \cdot \mathcal{P}_\Gamma \nabla\varphi|\nabla\phi| = \int_\Omega s\varphi|\nabla\phi|. \tag{3.15}$$

3.2. Stabilization. It is known that the pure Galerkin scheme will not work for (3.15), especially for large $\boldsymbol{v}$. Here, we adopt the FCT methodology to construct a positivity preserving nonoscillatory numerical scheme for the reaction-diffusion-advection equation on a surface $\Gamma \subset \Omega^d$, when $d = 2, 3$. We would like to note that the equation (3.15) can be stabilized by the FCT approach and then coupled in a segregated way with the equation (2.1), which in turn might be also stabilized with the FCT (or any other convection-related) algorithm. This allows to treat numerically the interaction of in-a-domain defined entities with on-a-surfaces defined ones.

Given a set of piecewise-polynomial basis functions $\{\varphi_i\}$ and a time step Δt, the standard

Galerkin discretization in space together with the implicit Euler discretization in time yields the following linearized algebraic equation

$$[\boldsymbol{M}(|\nabla\phi|) + \Delta t\boldsymbol{L}(D|\nabla\phi|) - \Delta t\boldsymbol{K}(\boldsymbol{v}^n|\nabla\phi|)]\,\rho^{n+1} = \boldsymbol{M}(|\nabla\phi|)\rho^n + \Delta t s^n(|\nabla\phi|), \tag{3.16}$$

where ρ^{n+1} is the unknown density of species at time t_{n+1}. Here, $\boldsymbol{M}(\cdot)$ denotes the (consistent) mass matrix, $\boldsymbol{L}(\cdot)$ is the discrete Laplace-Beltrami operator, and $\boldsymbol{K}(\cdot)$ is the discrete on-surface advection operator with entries defined by the formulae

$$m_{ij}(\psi) = \int_\Omega \varphi_i\varphi_j\psi, \tag{3.17}$$

$$l_{ij}(\psi) = \int_\Omega P_\Gamma\nabla\varphi_i\cdot\nabla\varphi_j\psi, \tag{3.18}$$

$$k_{ij}(\boldsymbol{\psi}) = \int_\Omega \varphi_i\boldsymbol{\psi}\cdot P_\Gamma\varphi_j, \tag{3.19}$$

$$s_i^n(\psi) = \int_\Omega \varphi_i s_i\psi. \tag{3.20}$$

As shown by Kuzmin *et al.* [27, 28, 29], positivity constraints can be readily enforced at the discrete level using a conservative manipulation of the matrices $\boldsymbol{M}$ and $\boldsymbol{K}$, supposing that the source term $\Delta t s^n$ does not course any threat to positivity. The former is approximated by its diagonal counterpart $\boldsymbol{M}_L$ constructed using row-sum mass lumping

$$\boldsymbol{M}_L := \text{diag}\{m_i\}, \qquad m_i = \sum_j m_{ij}(|\nabla\phi|). \tag{3.21}$$

Next, all negative off-diagonal entries of $\boldsymbol{K}$ are eliminated by adding an artificial diffusion operator $\boldsymbol{D}$. For conservation reasons, this matrix must be symmetric with zero row and column sums. For any pair of neighboring nodes i and j, the entry d_{ij} is defined as [27, 28]

$$d_{ij} = \begin{cases} \max\{-k_{ij}, 0, -k_{ji}\}, & j \neq i, \\ -\sum_{k\neq i} d_{ik}, & j = i. \end{cases} \tag{3.22}$$

It is clear that $d_{ij} = d_{ji}$. The result is a positivity-preserving discretization of low order. By construction, the difference f between the residual of this scheme and that of the underlying Galerkin approximation

$$f = (\boldsymbol{M}_L - \boldsymbol{M}(|\nabla\phi|))\,\frac{u^{n+1}-u^n}{\Delta t} - \boldsymbol{D}\,u^{n+1} \tag{3.23}$$

admits a conservative decomposition into a sum of skew-symmetric antidiffusive fluxes

$$f_i = \sum_{j\neq i} f_{ij}, \qquad f_{ji} = -f_{ij}, \qquad \forall j \neq i. \tag{3.24}$$

To achieve high resolution while keeping the scheme positivity-preserving, each flux is multiplied by a solution-dependent correction factor $\alpha_{ij} \in [0, 1]$ and is inserted into the right-hand side of the nonoscillatory low-order scheme. The original Galerkin discretization corresponds to the setting $\alpha_{ij} := 1$. It may be used in regions where the numerical solution is smooth and well-resolved. The setting $\alpha_{ij} := 0$ is appropriate in the neighborhood of steep fronts.

In essence, the off-diagonal entries of the sparse matrices $\boldsymbol{M}$ and $\boldsymbol{K}$ are replaced by

$$m_{ij}^* := \alpha_{ij}m_{ij}, \qquad k_{ij}^* := k_{ij} + (1-\alpha_{ij})d_{ij},$$

while the diagonal coefficients of the flux-corrected Galerkin operators are given by

$$m_{ii}^* := m_i - \sum_{j\neq i} \alpha_{ij} m_{ij}, \qquad k_{ii}^* := k_{ii} - \sum_{j\neq i} (1-\alpha_{ij}) d_{ij}.$$

In implicit FEM-FCT schemes [29, 27, 28], the optimal values of α_{ij} are determined using Zalesak's algorithm [47]. The limiting process begins with cancelling all fluxes that are diffusive in nature and tend to flatten the solution profiles. The required modification is:

$$f_{ij} := 0 \qquad \text{if} \quad f_{ij}(u_j - u_i) > 0,$$

where u is a positivity-preserving solution of low order [29, 27, 28]. The remaining fluxes are truly antidiffusive, and the computation of α_{ij} involves the following algorithmic steps:

1. Compute the sums of positive/negative antidiffusive fluxes into node i

$$P_i^+ = \sum_{j\neq i} \max\{0, f_{ij}\}, \qquad P_i^- = \sum_{j\neq i} \min\{0, f_{ij}\}.$$

2. Compute the distance to a local extremum of the auxiliary solution u

$$Q_i^+ = \max\{0, \max_{j\neq i}(u_j - u_i)\}, \qquad Q_i^- = \min\{0, \min_{j\neq i}(u_j - u_i)\}.$$

3. Compute the nodal correction factors for the net increment to node i

$$R_i^+ = \min\left\{1, \frac{m_i\, Q_i^+}{\Delta t P_i^+}\right\}, \qquad R_i^- = \min\left\{1, \frac{m_i\, Q_i^-}{\Delta t P_i^-}\right\}.$$

4. Check the sign of the antidiffusive flux and apply the correction factor

$$\alpha_{ij} = \begin{cases} \min\{R_i^+,\, R_j^-\}, & \text{if } \ f_{ij} > 0, \\ \min\{R_i^-,\, R_j^+\}, & \text{otherwise.} \end{cases}$$

For practical implementation details, we refer to the original publications by Kuzmin *et al.* [29, 27, 28].

Due to the level-set methodology and the algebraic nature of the flux-corrected schemes, TVD and some FCT methods can be implemented for the equation (3.15) almost without changes (one should only operate with proper $\boldsymbol{M}(\cdot)$, $\boldsymbol{L}(\cdot)$ and $\boldsymbol{K}(\cdot)$ matrices). Nevertheless, there are certain FCT schemes which necessiate the evaluation of ρ_{x_i} during the antidiffusive flux-limiting, e.g. *Gradient-based slope limiting* in [30]. In this case the corresponding projection onto the tangential space $\mathcal{T}_{\boldsymbol{x}}\Gamma$ is required. Numerical tests showed that the TVD scheme drops behind the FCT algorithms in accuracy: neglecting the $(\boldsymbol{M}_L - \boldsymbol{M}(|\nabla\phi|))\,\dfrac{\rho^{n+1}-\rho^n}{\Delta t}$ term results in a smeared solution. Therefore, the FCT-based algorithms are in this case more preferable.

4. Numerical results. In this section we demonstrate that the proposed level-set technique together with the algebraic flux correction makes it possible to perform numerical simulations of chemotaxis processes on surfaces of nonzero curvature. Here, we consider chemotaxis models with blow-ups on a sphere and an ellipsoid, as well as pattern-forming dynamics of cells on a sphere with the Fischer overcrowding-prevention term. In every case the solver was able to deliver plausible, nonoscillatory and sufficiently accurate numerical solutions.

4.1. Blow-up on a sphere. As a first example, we consider the minimal Keller-Segel model on a sphere $\Gamma = \{\boldsymbol{x} \,:\, |\boldsymbol{x}| = 5\} \subset \Omega = \{\boldsymbol{x} \,:\, 4.0 \leq |\boldsymbol{x}| \leq 6.0\}$:

$$\partial_t \rho_1 = \Delta_\Gamma \rho_1 - \chi \nabla \cdot (\rho_1 \nabla_\Gamma \rho_2), \tag{4.1}$$

$$\partial_t \rho_2 = \Delta_\Gamma \rho_2 - \rho_2 + \rho_1 \tag{4.2}$$

with the following bell-shaped initial conditions

$$\rho_1(x_1, x_2, x_3, t = 0) = 5.0\, e^{-0.5\left((x_1-5.0)^2+x_2^2+x_3^2\right)},$$
$$\rho_2(x_1, x_2, x_3, t = 0) = 5.0\, e^{-0.5\left((x_1-5.0)^2+x_2^2+x_3^2\right)}.$$

We use a uniform grid with trilinear finite elements with $393\,216$ cells and $798\,980$ d.o.f. More on the mesh construction one can find in the following subsection 4.3. The time step is $\Delta t = 10^{-4}$ and the chemosensitivity $\chi = 50$. The level-set function is chosen to be $\phi = \sqrt{x_1^2 + x_2^2 + x_3^2} - 5.0$. It is known, that the stability in terms of blow-up of the system (4.1)-(4.2) crucially depends on the chemoattractant sensitivity χ. By fixing all involved parameters and varying the magnitude of χ one can make either the diffusion processes or the chemoattractive transport of cells dominant. The former situation leads to steady-state solutions, whereas the latter gives rise to evolving in time solutions, blow-ups etc. For our parameter setting we would expect a blow-up in finite time of the cell density ρ_1 and the chemoattractant concentration ρ_2, if ρ_1 and ρ_2 live on a 2D-plane. From figures (4.2(a))–(4.2(d)) one observes that the numerical simulation of the system (4.1)–(4.2) leads also to an infinite growth of the initial peak of ρ_1 and, hence, ρ_2.

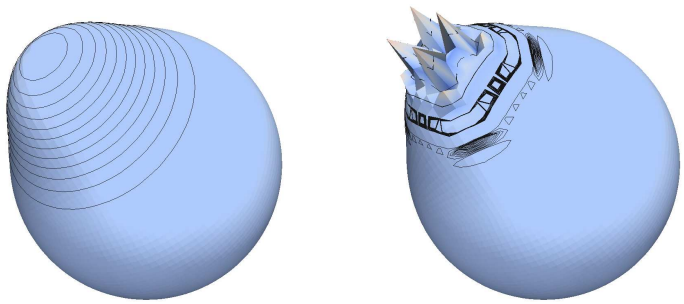

(a) initial (b) $t = 0.01$

FIG. 4.1. *Blow-up on a sphere, pure Galerkin scheme. One observes wiggles in a solution profile.*

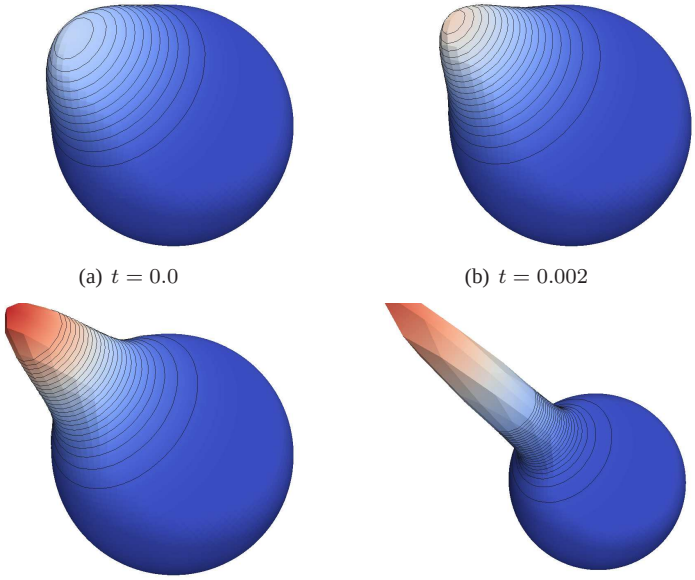

(a) $t = 0.0$ (b) $t = 0.002$

(c) $t = 0.005$ (d) $t = 0.01$

FIG. 4.2. *Blow-up on a sphere, FCT scheme. The screenshots were taken at times* $t = 0.0, 0.002, 0.005, 0.01$.

For the pure Galerkin discretization (i.e., without any stabilization) of the problem (4.1)–(4.2) the cell density u becomes negative at a certain intermediate level. The nonphysical negative values grow rapidly as time evolves, which leads to an abnormal termination of the simulation run, see figures 4.1(a)–4.1(b). At the same time, the FCT stabilization technique preserves positivity and smoothness of the solution.

4.2. Blow-up on an ellipsoid. Let us consider a minimal Keller-Segel model

$$\partial_t \rho_1 = \Delta_\Gamma \rho_1 - \chi \nabla \cdot (\rho_1 \nabla_\Gamma \rho_2), \tag{4.3}$$

$$\partial_t \rho_2 = \Delta_\Gamma \rho_2 - \rho_2 + \rho_1 \tag{4.4}$$

with the bell-shaped initial conditions

$$\rho_1(x_1, x_2, x_3, t = 0) = 5.0\, e^{-0.4\left((x_1-2.41459)^2+(x_2-2.41459)^2+(x_3-2.41459)^2\right)},$$

$$\rho_2(x_1, x_2, x_3, t = 0) = 5.0\, e^{-0.4\left((x_1-2.41459)^2+(x_2-2.41459)^2+(x_3-2.41459)^2\right)}.$$

The main point of this kind of numerical experiments is to understand if the position of the blow-up depends on the curvature or not. Here, we show an exemplary test configuration, when $\Gamma = \{\boldsymbol{x} \,:\, x_1^2/9 + x_2^2/25 + x_3^2/49 = 1\}$. The point $\boldsymbol{x} = (2.41459, 2.41459, 2.41459)^T \in \Gamma$ of the center of initial peaks has different curvatures in x_1-, x_2- and x_3-directions. We choose $\chi = 50$ and $\Delta t = 1.0^{-4}$. In figures 4.3(a)-4.3(d) one can see various levels of the ellipsoidal mesh. Here we like to mention that all our meshes enjoy favorable properties by courtesy of our colleague Jens F. Acker. The final mesh for the numerical simulation is the 7th level of the refinement and it consists of $98\,304$ cells and $245\,780$ d.o.f.

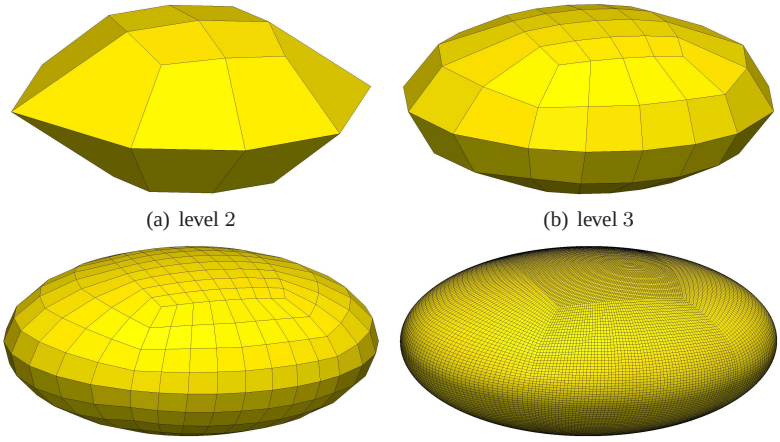

(a) level 2 (b) level 3

(c) level 4 (d) level 7

FIG. 4.3. *Ellipsoidal mesh, various levels of refinement.*

Figures 4.4(a)–4.4(d) display the evolution of the peak for the FCT application at some time instances. One can observe that the peak rises in magnitude, while its support decreases in size. The numerical blow-up is reached in a finite time, but no change of the position of the peak is detected.

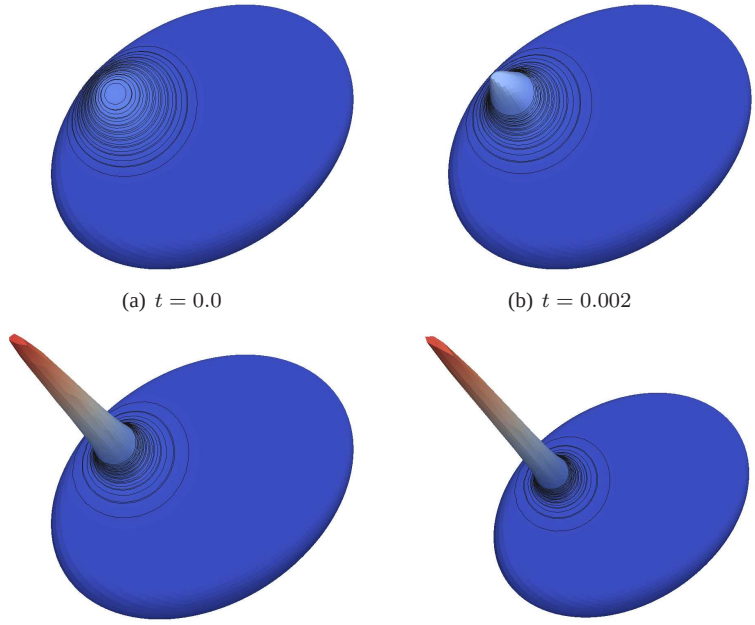

(a) $t = 0.0$ (b) $t = 0.002$

(c) $t = 0.005$ (d) $t = 0.006$

FIG. 4.4. *Blow-up on an ellipsoid, FCT scheme. The screenshots were taken at times* $t = 0.0, 0.002, 0.005, 0.006$.

4.3. Pattern-formation on a sphere. In the last example, we show coupling of a surface-defined equation with an equation, which is defined in the whole domain Ω. For this reason,

we modify the Mimura-Tsujikawa model [32, 38, 39], which describes the propagation of motile cells of *Escherichia coli*, in such a way that the cell density u travels along a membrane $\Gamma \subset \Omega$, while the chemoattractant c lives in Ω, e.g.

$$\partial_t \rho_1 = 0.0625 \Delta_\Gamma \rho_1 - 8.5 \nabla \cdot (\rho_1 \nabla_\Gamma c) + \rho_1 (1 - \rho_1) \quad \text{on} \ \ \Gamma \tag{4.5}$$

$$c_t = \Delta c - 32.0 c + {\rho_1}^* \quad \text{in} \quad \Omega, \tag{4.6}$$

where ${\rho_1}^*$ is a natural extension of ρ_1 to Ω. Initial conditions are chosen as follows

$$\rho_1(\boldsymbol{x}, t = 0) = 1 + \sigma(\boldsymbol{x}),$$
$$c(\boldsymbol{x}, t = 0) = 1/32,$$

where $\sigma(\boldsymbol{x})$ is defined as

$$\sigma(\boldsymbol{x}) = \begin{cases} 0.2, & \text{if} \quad \|\boldsymbol{x} - (5, 0, 0)^T\| \leq 1.5, \\ 0, & \text{otherwise}. \end{cases}$$

We prescribe zero-flux boundary conditions on $\partial\Omega$ for c and ρ^*. As a domain we take $\Omega = \{\boldsymbol{x} \ : \ 4.8 \leq |\boldsymbol{x}| \leq 5.2\}$ and $\Gamma = \{\boldsymbol{x} \ : \ |\boldsymbol{x}| = 5\}$, which is defined by the zero level of the level-set function $\phi = \sqrt{x_1^2 + x_2^2 + x_3^2} - 5.0$. During construction of the corresponding mesh we exploit that the manifold Γ is prescribed and stationary. Taking a coarse quad mesh of a unit sphere, we refine it along Γ a given number of times. The generated nodes were then copied and scaled to the given radii to form several levels. The node numbers for each of these levels correspond by a shift by an integer multiple of the number of nodes on the manifold. This made it easy to create the hexahedral cells of these levels as extrusions of the original quad cells. The resulting mesh consists of $786\,432$ cells, that corresponds to $1\,671\,236$ d.o.f. The mesh has a good refinement in the Γ-direction, which makes it possible to capture the dynamics of the cell density ρ_1 in a best possible way. In figures 4.5(a)-4.5(c) one can see three successive refinement levels.

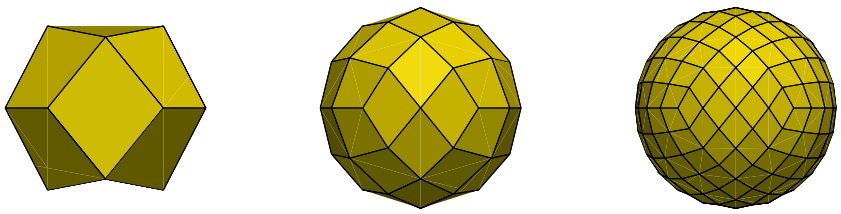

(a) level 1 (b) level 2 (c) level 3

FIG. 4.5. *Spherical mesh for three successive levels of refinement.*

Our code is able to capture the complex dynamics of the cell density. As reported in [38, 39] for the case, when $\rho_1 \in \Omega^d$, $d = 2, 3$, we observe a similar behavior, but now on a sphere. Namely, placed in a point $\boldsymbol{x} = (5, 0, 0)^T$, the initial concentration of bacteria propagates along Γ in a moving wave-pattern as a response to the chemosensitivity, see figures 4.6(a)-4.6(f). Here, the FCT method works well to preserve *smoothness* and positivity of the cell density.

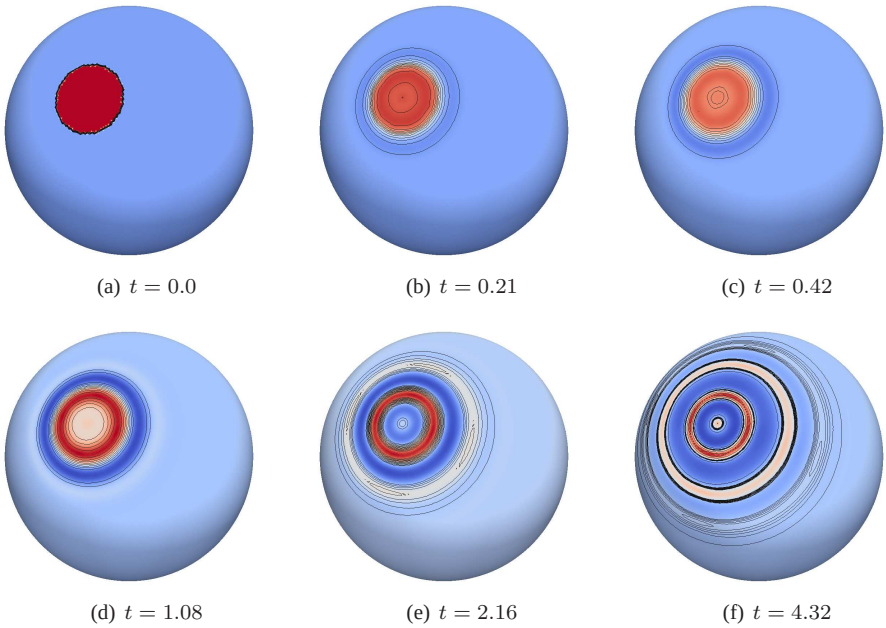

(a) $t = 0.0$ (b) $t = 0.21$ (c) $t = 0.42$

(d) $t = 1.08$ (e) $t = 2.16$ (f) $t = 4.32$

FIG. 4.6. *Pattern formation on a sphere. The screenshots were taken at times* $t = 0.0, 0.21, 0.42, 1.08, 2.16, 4.32$, $\Delta t = 0.01$.

5. Conclusions. The previously constructed algorithmical framework for chemotaxis models in 2 and 3 spatial dimensions, see [38, 39], was extended to chemotaxis-related equations, which are defined on a smooth closed and oriented surface $\Gamma \subset \Omega^d$, $d = 2, 3$. The level set method was used to implicitly describe the surface Γ and to construct a numerical scheme for corresponding partial differential equations. Then, we applied the linearized flux-corrected FEM transport algorithm to preserve positivity and to guarantee the nonoscillatory of the resulting solution. The demonstrated numerical results show that the constructed scheme is sufficiently robust and can deliver a suitable solution for chemotaxis-like models, both on a surface and/or in a domain.

In future, a peculiar numerical and mathematical analysis for gradient-based slope limiters for the partial differential equations on surfaces is desired. We are optimistic that this is a very promising stabilization method for the numerical treatment of surface-based chemotaxis problems in medicine and biology.

The proposed numerical scheme can be used to give an instinctive glance on so far open analytical questions such as the relation between the blow-up phenomena (blow-up time, location of the blow-up, etc.) and the curvature of the underlying manifold. We hope that the corresponding numerical experiments can shed light onto these questions, which might serve to extend, deepen and improve the theory of chemotaxis-driven models.

The last trends in the mathematical modeling for bio-processes show the importance of partial differential equations on evolving in time surfaces $\Gamma(t)$. For example, these kind of processes arise when one considers reaction and interaction of some entities (e.g., proteins, chemicals, etc.) on a membrane of a cell [5], there the evolution of a membrane is due to its response on the distribution of some substances along its surface. Here, one has to take into account not only advective terms, which are due to chemotaxis effects, transport and external flows, but also those, which are due to the time-evolution of Γ. The current work can serve as a pre-validation and preparation step for this class of applications.

Aknowledgment.

- The authors would like to thank Prof. Dr. T. Hillen for a fruitful discussion, posted questions and his valuable comments.
- Robert Strehl is supported by a PhD scholarship of TU Dortmund.

REFERENCES

[1] M. AIDA, T. TSUJIKAWA, M. EFENDIEV, A. YAGI AND M. MIMURA, *Lower estimate of the attractor dimension for a chemotaxis growth system*, J. London Math. Soc. **74**, no. 2, pp. 453–474, 2006.

[2] M. AIDA AND A. YAGI, *Target pattern solutions for chemotaxis-growth system*, Scientiae Mathematicae Japonicae **59**, no. 3, pp. 577–590, 2004.

[3] D. AMBROSI, F. BUSSOLINO, L. PREZIOSI, *A review of vasculogenesis models*, Computational and Mathematical Methods in Medicine: An Interdisciplinary Journal of Mathematical, Theoretical and Clinical Aspects of Medicine, 1748-6718, **6**, no. 1, pp. 1–19, 2005.

[4] A. R. A. ANDERSON, M A. J. CHAPLAIN, E. L. NEWMAN, R. J. C. STEELE AND A. M. THOMPSON, *Mathematical modelling of tumour invasion and metastasis*, Journal of Theoretical Medicine **2**, pp. 129–154, 1999.

[5] M. BERGDORF, I. F. SBALZARINI, P. KOUMOUTSAKOS, *A Lagrangian particle method for reaction-diffusion systems on deforming surfaces*, J. Math. Biol., Vol. **61** (5), pp. 649–663, 2009.

[6] M. A. J. CHAPLAIN, *The mathematical modelling of tumour angiogenesis and invasion*, ACTA Biotheoretica, Vol. **43** (4), pp. 387–402, 1995.

[7] M. A. J. CHAPLAIN, *Continuous and discrete mathematical models of tumor-induced angiogenesis*, Bulletin of Mathematical Biology, Vol. **60**, pp. 857–900, 1998.

[8] M. A. J. CHAPLAIN, *Mathematical modelling of angiogenesis*, Journal of Neuro-Oncology, Vol. **50**, pp. 37–51, 2000.

[9] M. A. J. CHAPLAIN, A. M. STUART, *A model mechanism for the chemotactic response of endothelial cells to tumour angiogenesis factor*, IMA Journal of Mathematics Applied in Medicine and Biology, Vol. **10**, pp. 149–168, 1993.

[10] A. CHERTOCK AND A. KURGANOV, *A second-order positivity preserving central-upwind scheme for chemotaxis and haptotaxis models*, Numer. Math., **111:169–205**, 2008.

[11] L. CORRIASA, B. PERTHAME AND H. ZAAG, *Global solutions of some chemotaxis and angiogenesis systems in high space dimensions*. Milan J. Math. **72**, pp. 1–28, 2004.

[12] L. CORRIASA AND B. PERTHAME, *Asymptotic decay for the solutions of the parabolic Keller-Segel chemotaxis system in critical spaces*. Mathematical and Computer Modelling **47**, pp. 755–764, 2008.

[13] G. DZIUK, C. M. ELLIOTT, *Eulerian finite element method for parabolic PDEs on implicit surfaces*, Interfaces and Free Boundaries, **10**, pp. 399–415, 2008.

[14] Y. EPSHTEYN, *Discontinuous Galerkin methods for the chemotaxis and haptotaxis models*, J. Comput. Appl. Math. **224**, no. 1, pp. 168–181, 2009.

[15] Y. EPSHTEYN AND A. KURGANOV, *New interior penalty discontinuous Galerkin methods for the Keller-Segel chemotaxis model*, SIAM J. Numer. Anal. **47**, no. 1, pp. 386–408, 2008.

[16] F. FILBET, *A finite volume scheme for the Patlak-Keller-Segel chemotaxis model*, Numer. Math. **104**, no. 4, 457–488, 2006.

[17] H. GAJEWSKI, W. JÄGER AND A. KOSHELEV, *About loss of regularity and 'blow up' of solutions for quasilinear parabolic systems*, R-Report, Institut fuer Angewandte Analysis und Stochastik (IAAS), Berlin (Germany), 1993.

[18] H. GAJEWSKI AND K. ZACHARIAS, *Global behavior of a reaction-diffusion system modelling chemotaxis*, Math. Nachr. **195**, pp. 77–114, 1998.

[19] A. GAMBA, D. AMBROSI, A. CONIGLIO, A. DE CANDIA, S. DI TALIA, E. GIRAUDO, G. SERINI, L. PREZIOSI, AND F. BUSSOLINO, *Percolation, morphogenesis, and Burgers dynamics in blood vessels formation*, Phys. Rev. Lett. **90**, 118101.

[20] D. HORSTMANN, *Generalizing the Keller-Segel Model: Lyapunov Functionals, Steady State Analysis, and Blow-Up Results for Multi-species Chemotaxis Models in the Presence of Attraction and Repulsion Between Competitive Interacting Species*, J. Nonlinear Sci. **21**, pp. 231–270, 2011.

[21] D. HORSTMANN AND M. LUCIA, *Uniqueness and symmetry of equilibria in a chemotaxis model*, Journal für die Reine und angewandte Mathematik (Crelle's Journal) **654**, pp. 83 – 124, 2011.

[22] D. HORSTMANN AND G. WANG, *Blow-up in a chemotaxis model without symmetry assumptions*, European Journal of Applied Mathematics **12**, pp. 159–177, 2001.

[23] D. HORSTMANN AND M. WINKLER, *Boundedness vs. blow-up in a chemotaxis system*, Journal of Differential Equations **215**, pp. 52–107, 2004.

[24] E. KELLER AND L. SEGEL, *Initiation of slime mold aggregation viewed as an instability*, J. Theor. Biol.,

26:399–415, 1970.
[25] E. KELLER AND L. SEGEL, *Model for chemotaxis*, J. Theor. Biol., **30:225–234**, 1971.
[26] D. KUZMIN, R. LÖHNER AND S. TUREK, *Flux-Corrected Transport*, Springer, 2nd edition, 978-94-077-4037-2, 2012.
[27] D. KUZMIN AND M. MÖLLER, *Algebraic flux correction I. Scalar conservation laws*, in: D. KUZMIN, R. LÖHNER, S. TUREK (Eds.), *Flux-Corrected Transport: Principles, Algorithms, and Applications*, Springer, Berlin, 2005, pp. 155–206.
[28] D. KUZMIN AND S. TUREK, *Flux correction tools for finite elements*, J. Comput. Phys., **175:525–558**, 2002.
[29] D. KUZMIN, *Explicit and implicit FEM-TVD algorithms with flux linearization*, J. Comput. Phys., **228:2517–2534**, 2009.
[30] D. KUZMIN, *Linearity-preserving flux correction and convergence acceleration for constrained Galerkin schemes*, Journal of Computational and Applied Mathematics, **236:2317–2337**, 2012.
[31] R. J. LEVEQUE, *Wave propagation algorithms for multi-dimensional hyperbolic systems*, J. Comput. Phys. **131**, pp. 327–353, 1997.
[32] M. MIMURA AND T. TSUJIKAWA, *Aggregating pattern dynamics in a chemotaxis model including growth*, Physica A **230**, pp. 499–543, 1996.
[33] T. NAGAI, *Blowup of nonradial solutions to parabolic-elliptic systems modeling chemotaxis in two-dimensional domains*, J. Inequal. Appl. **6**, pp. 37–55, 2001.
[34] K. OSAKI AND A. YAGI, *Finite dimensional attractors for one-dimensional Keller-Segel equations*. Funkcialaj Ekvacioj **44**, pp. 441–469, 2001.
[35] N. SAITO, *Conservative upwind finite-element method for a simplified Keller-Segel system modelling chemotaxis*, IMA J. Numer. Anal., **27**, pp. 332–365, 2007.
[36] T. SENBA AND T. SUZUKI, *Parabolic System of Chemotaxis: Blowup in a Finite and the Infinite Time*, Methods Appl. Anal. **8**, pp. 349–368, 2001.
[37] G. SERINI, D. AMBROSI,E. GIRAUDO, A. GAMBA, L. PREZIOSI AND F. BUSSOLINO, *Modeling the early stages of vascular network assembly*, The EMBO Journal **22**, pp. 1771–1779, 2003.
[38] R. STREHL, A. SOKOLOV, D. KUZMIN AND S. TUREK, *A flux-corrected finite element method for chemotaxis problems*, Computational methods in applied mathematics **10**, no. 2, pp. 219–232, 2010.
[39] R. STREHL, A. SOKOLOV, D. KUZMIN, D. HORSTMANN AND S. TUREK, *A positivity-preserving finite element method for chemotaxis problems in 3D*, accepted to the Journal of Computational and Applied Mathematics, 2012.
[40] R. STREHL, A. SOKOLOV AND S. TUREK, *Efficient, accurate and flexible Finite Element solvers for Chemotaxis problems*, Computers and Mathematics with Applications **34**, no. 3, pp. 175–189, 2011.
[41] S. TUREK, *Efficient Solvers for Incompressible Flow Problems: An Algorithmic and Computational Approach*. Springer, Berlin, 1999.
[42] R. TYSON, S. R. LUBKIN AND J. D. MURRAY, *A minimal mechanism for bacterial pattern formation*, Proc. R. Soc. Lond. B **266**, pp. 299–304, 1999.
[43] R. TYSON, S. R. LUBKIN AND J. D. MURRAY, *Model and analysis of chemotactic bacterial patterns in a liquid medium*, J. Math. Biol. **38**, pp. 359–375, 1999.
[44] R. TYSON, L. G. STERN AND R. J. LEVEQUE, *Fractional step methods applied to a chemotaxis model*, J. Math. Biol. **41**, pp. 455–475, 2000.
[45] C. M. ELLIOTT, B. STINNER AND C. VENKATARAMAN, *Modelling cell motility and chemotaxis with evolving surface finite elements*, J. R. Soc. Interface, PMID: 22675164, 2012.
[46] C. LANDSBERG, F. STENGER, A. DEUTSCH, M. GELINSKY, A. RÖSEN-WOLFF AND A. VOIGT, *Chemotaxis of mesenchymal stem cells within 3D biomimetic scaffolds–a modeling approach.*, J. Biomech. **44**(2), pp. 359–364, 2011.
[47] S. T. ZALESAK, *Fully multidimensional flux-corrected transport algorithms for fluids*, J. Comput. Phys., **31:335–362**, 1979.